

The Relationship of Hard X-ray and Optical Line Emission in Low Redshift Active Galactic Nuclei

T. M. Heckman¹, A. Ptak¹, A. Hornschemeier^{1,2}, G. Kauffmann³

heckman@pha.jhu.edu

ABSTRACT

In this paper we assess the relationship of the population of Active Galactic Nuclei (AGN) selected by hard X-rays to the traditional population of AGN with strong optical emission lines. First, we study the emission-line properties of a new hard X-ray selected sample of 47 local AGN (classified optically as both Type 1 and Type 2 AGN). We find that the hard X-ray (3-20 keV) and [OIII] λ 5007 optical emission-line luminosities are well-correlated over a range of about four orders-of-magnitude in luminosity (mean luminosity ratio 2.15 dex with a standard deviation of $\sigma = 0.51$ dex). Second, we study the hard X-ray properties of a sample of 55 local AGN selected from the literature on the basis of the flux in the [OIII] line. The correlation between the hard X-ray (2-10 keV) and [OIII] luminosity for the Type 1 AGN is consistent with what is seen in the hard X-ray selected sample. However, the Type 2 AGN have a much larger range in the luminosity ratio, and many are very weak in hard X-rays (as expected for heavily absorbed AGN). We then compare the hard X-ray (3-20 keV) and [OIII] luminosity functions of AGN in the local universe. These have similar faint-end slopes with a luminosity ratio of 1.60 dex (0.55 dex smaller than the mean value for individual hard X-ray selected AGN). We conclude that at low redshift, selection by narrow optical emission-lines will recover most AGN selected by hard X-rays (with the exception of BL Lac objects). However, selection by hard X-rays misses a significant fraction of the local AGN population with strong emission lines.

Subject headings: Galaxies: active — Galaxies: Seyfert — Galaxies: Quasars — Galaxies: X-rays

¹Center for Astrophysical Sciences, Department of Physics & Astronomy, Johns Hopkins University, Baltimore, MD 21218

²Laboratory for High Energy Astrophysics, NASA Goddard Space Flight Center, Greenbelt, MD 20771

³Max Planck Institut für Astrophysik, D-85748 Garching, Germany

1. Introduction

One of the fundamental properties of Active Galactic Nuclei (AGN) that sets them apart from stars and galaxies is the very broad-band nature of their intrinsic spectral energy distribution. In Type 1 AGN where we have a clear view of the “central engine”, there is a comparable amount of energy radiated per decade in frequency over a span of more than six orders-of-magnitude in photon energy from the far-infrared to hard X-rays (e.g. Elvis et al. 1994). The panchromatic nature of AGN is both a blessing and a curse. It enables us to find and then investigate AGN with a broad array of facilities, but this very diversity implies that any single technique may provide a biased perspective (e.g. Mushotzky 2004). In this paper we address this issue in the context of local samples of AGN selected by their hard X-ray emission, compared to AGN with strong optical emission-lines.

This particular comparison is very timely. On the one hand, “mega surveys” like the 2dF Galaxy Redshift Survey (Colless et al. 2001), the 2dF QSO Redshift Survey (Croom et al. 2004), and the Sloan Digital Sky Survey (SDSS -York et al. 2000) are generating samples of hundreds of thousands of AGN identified on the basis of their optical spectroscopic properties. These data not only allow AGN to be efficiently recognized (e.g. Kauffmann et al 2003; Hao et al. 2005a; Zakamska et al. 2003), but the same data can be used to quantify many of the key properties of the AGN and their host galaxies (e.g. Kauffmann et al. 2003). Recently, Heckman et al. (2004) have used the SDSS data to show that the population of low mass black holes in the present day universe is growing at a substantial rate, and that the co-construction of black holes and bulges is linked today. To what extent are these results affected by the use of optical emission lines to identify and quantify the AGN? For example, radio- selected AGN in the SDSS are associated with a very different population (the most massive black holes and giant elliptical galaxies - Best et al. 2005a,b).

On the other hand, the deep X-ray surveys carried out by the Chandra X-ray Observatory have revolutionized our picture of the cosmic history of the AGN phenomenon and thus of the growth of supermassive black holes (e.g. Ueda et al. 2003; Barger et al. 2005 - hereafter B05; Hasinger et al. 2005). These results show that a substantial fraction of the growth of supermassive black holes as traced by hard X-ray emission has occurred relatively recently (since $z \sim 1$), and that this late growth has preferentially occurred in AGN of low or moderate luminosity. It is reassuring that these results appear compatible with the inferences drawn from the SDSS sample of emission-line AGN, at least qualitatively. However, the relationship between AGN selected via hard X- ray emission and optical emission lines is still murky.

While the most luminous hard-X-ray-selected AGN are usually identified optically with quasars, most of the lower luminosity objects are not. There have been several explanations

for this. The most revolutionary possibility (Steffen et al. 2003; B05) is that these lower luminosity objects are a genuinely new type of AGN that intrinsically lacks the strong UV and optical continuum and associated Broad Line Region that defines Type 1 AGN. The second and most mundane explanation is that this is just “aperture dilution”: at the redshifts of these AGN the slit of the optical spectrograph encompasses a large fraction of the entire AGN host galaxy and the observed light is dominated by the host galaxy except in the case of the most powerful AGN. This makes it difficult to recognize the presence of an AGN (Moran, Filippenko, & Chornock 2002).

The final possibility (e.g. B05) is that these are normal AGN that are dust-obscured at optical and ultraviolet wavelengths, but that this obscuring material is easily penetrated by hard X-rays (absorbing column $< 10^{23} \text{ cm}^{-2}$). The widespread existence of obscured AGN has been known since it was realized over twenty years ago (Lawrence & Elvis 1982; Antonucci & Miller 1985; Krolik & Begelman 1988) that Type 1 and Type 2 AGN could be unified. In a Type 1 (Type 2) AGN our line of sight is near the polar axis (equatorial plane) of a dusty toroidal structure that surrounds the central engine (black hole plus accretion disk). The torus is optically-thick to visible and ultraviolet photons emitted by the central engine, but (in many AGN) is optically thin to hard X-rays (e.g. Risaliti, Maiolino, & Salvati 1999). To reconcile this picture with the results from the hard X-ray surveys would require that the “covering fraction” of the obscuring torus increases systematically with decreasing hard X-ray luminosity (Ueda et al. 2003; B05).

It has been difficult to decisively discriminate between the above possibilities, largely because the samples of hard X-ray selected AGN have mostly come from deep surveys that cover relatively small solid angles. As a result the AGN and their host galaxies are relatively faint and distant, making it difficult to investigate them in detail.

In this paper we will use existing catalogs to compare the properties of AGN selected by hard X-rays to those with bright optical emission lines. In section 2 we will describe a new “all-sky” sample of 95 relatively nearby AGN detected serendipitously in the 3-20 keV hard X-ray band in the Rossi X-ray Timing Experiment slew survey (Revnivtsev et al. 2004; Sazonov & Revnivtsev 2004) and also a sample derived from extensive compilations of AGN [OIII] λ 5007 emission-line properties (Xu, Livio, & Baum 1999; Whittle 1992). In section 3 we will compare the relationship between the hard X-ray and [OIII] luminosities for these two samples. In section 4 we will compare the hard X-ray and [OIII] luminosity functions for AGN in the local universe. In section 5, we will examine the dependence of the ratio of Type 1 and Type 2 AGN on their hard X-ray luminosity. Finally, we will summarize our results and their implications in section 6.

2. AGN Samples

2.1. AGN Selected by Hard X-rays

Sazonov & Revnivtsev (2004 - hereafter SR04) have provided optical identifications and hard X-ray luminosities (in the 3 to 20 keV band) for 95 AGN detected in the RXTE slew survey (XSS). The XSS covered 90% of the sky at $|b| > 10^\circ$ to a flux limit in the 3-20 keV band of 2.5×10^{-11} erg s $^{-1}$ cm $^{-2}$ or better. There are 35 sources in the XSS that are not identified optically, and based on their X-ray spectra these are likely to be AGN. The XSS provides positions to only $\sim 1^\circ$ accuracy, so additional follow-up hard X-ray observations will be required to identify these sources. In the Northern celestial hemisphere where the optical catalogs used for cross-identification are more extensive, there are 45 identified AGN and only 4 unidentified sources. Thus, the SR04 sample provides a reliable census of the sources that dominate the AGN population at relatively bright hard X-ray flux levels.

The SR04 sample has a median redshift of $z \sim 0.035$, but extends out to $z = 2.70$. Since our goal in this paper is to compare AGN populations in the local universe, we restrict the SR04 sample to $z < 0.2$. This eliminates only eight objects. The sample then consists of 65% Type 1 AGN (Type 1 Seyfert nuclei, quasars, and broad line radio galaxies), 22%, Type 2 AGN (Type 2 Seyferts and narrow line radio galaxies), and 13% BL Lacs. Given that 92% of the northern sample is identified, one immediate conclusion is that at most 8% of the hard X-ray selected objects would not be otherwise recognized as AGN. We emphasize that because of the low median redshift of this sample, aperture effects in the optical spectra will be small (e.g. Kewley, Jansen, & Geller 2005; Kauffmann et al. 2003). The optical spectroscopic signature of the AGN would be more difficult to detect if these AGN were at higher redshift.

2.2. AGN with Bright [OIII] Emission Lines

In the standard “unified model” for AGN (e.g. Antonucci 1993; Urry & Padovani 1995), narrow (FWHM \sim several hundred km/s) optical emission lines arise in gas located several hundred pc or more from the central engine and are excited by ionizing radiation escaping along the polar axis of the obscuring torus. Since this material lies outside the region of high gas column density (the torus), the narrow optical emission lines suffer only moderate amounts of dust obscuration (e.g. Dahari & De Robertis 1988; Keel et al. 1994; Kauffmann et al. 2003), even in cases in which the central hard X-ray source is almost totally obscured by a Compton-thick torus (e.g. Bassani et al. 1999). These narrow emission lines should therefore provide an unbiased orientation-independent indicator of the ionizing luminosity

of the central engine in both Type 1 and Type 2 AGN.

This concept has been validated empirically in several different studies of AGN (e.g. Mulchaey et al. 1994; Heckman 1995; Keel et al. 1994). As discussed extensively in Kauffmann et al. (2003), Heckman et al. (2004), and Brinchmann et al. (2004), the [OIII] λ 5007 line is the best optical estimator of the AGN power in Type 2 AGN, as it is the strongest narrow emission line in such AGN and the least contaminated by contribution from HII regions associated with star formation in the host galaxy.

Unfortunately, there is no all-sky catalog of AGN selected purely on the basis of their [OIII] λ 5007 flux (analogous to the SR04 hard X-ray sample). The best that we can do is to select from the known population of local AGN those objects with the brightest [OIII] emission lines. Xu, Livio, & Baum (1999 - hereafter X99) have published a catalog of [OIII] λ 5007 luminosities for 409 AGN. We have supplemented this with the similar catalog of 140 AGN compiled by Whittle (1992 - hereafter W92). These catalogs are not complete, and their members were originally discovered on the basis of a wide range of properties. While they should be representative of the [OIII]-bright local AGN population, there may well be biases in this sample compared to a ideal complete sample selected purely on the basis of [OIII] flux.

3. Comparison of Hard X-ray and [OIII] Properties

3.1. AGN Selected by Hard X-ray Emission

Of the 87 hard X-ray selected AGN in the SR04 catalog with $z < 0.2$, the union of the W92 and X99 optical emission line catalogs contains 47 (54%). These are listed in Table 1. The fraction of the SR04 sample in the merged X99 plus W92 catalogs is much higher in the northern sky (28 of 40, or 70%) compared to the south (19 of 47, or 40%).

While the SR04 Type 1 and Type 2 AGN populations are well represented in Table 1, this is not the case with the BL Lacs. BL Lacs comprise 13% of the SR04 sample, but none of these have [OIII] data in either X99 or W92. From the definition of a BL Lac object (e.g. Wolfe 1978), these will have generally have much weaker optical line emission than any of the other AGN classes in the SR04 catalog. We will keep this in mind in the discussion that follows. However, if we specifically exclude the BL Lac objects, then the fraction of AGN in the SR04 northern sample with [OIII] data in X99 or W92 is very high (28 of 33, or 85%). The corresponding fraction in the south is 19 of 43, or 44%.

Therefore, the high degree of completeness in the SR04 northern sample (92% identified

- see above) combined with the large fraction of these identified sources with [OIII] fluxes (85%) makes us confident that the northern component of the sample listed in Table 1 is representative of the optical properties of the local hard X-ray selected AGN population (with the important exception of BL Lac objects).

In Figure 1 we plot a histogram of the ratio $\log(L_{HX}/L_{OIII})$ for the AGN in Table 1. The distribution has a mean of 2.15 ± 0.08 dex (a factor of 140) and a standard deviation of 0.51 dex (a factor of 3.3). In Figure 2 we plot the hard X-ray *vs.* the [OIII] λ 5007 luminosity for this sample.¹ Note that in the cases of both [OIII] and hard X-rays, we have used the observed fluxes rather than fluxes corrected for intrinsic absorption. This is motivated by the main intent of our paper, which is to compare AGN selected on the basis of their *observed* properties. This is discussed further in the Appendix below.

By way of comparison, the distribution of the ratio of the optical continuum and [OIII] luminosity for optically selected Type 1 AGN in the SDSS has a standard deviation of 0.34 dex (see Heckman et al. 2004; Zakamska et al. 2003), while the distributions of the ratio of the 60 μ m and [OIII] luminosities for far-IR-selected Type 1 and Type 2 AGN both have standard deviations of ~ 0.5 dex (Keel et al. 1994).

To test the robustness of the result shown in Figures 1 and 2 we have subdivided the SR04 sample into Type 1 and Type 2 AGN. We find no significant difference in mean of the luminosity ratio (2.14 dex for Type 1 AGN *vs.* 2.17 dex for Type 2 AGN). As emphasized above, the SR04 sample is significantly more complete in the northern sky than in the south. Subdividing the sample into celestial hemispheres, we again find no significant difference in the mean luminosity ratio (2.11 dex in the north *vs.* 2.17 dex in the south).

3.2. AGN with Bright [OIII] Emission Lines

To construct a local AGN sample with a depth similar to the SR04 hard X-ray sample, we selected all AGN in the X99 or W92 catalogs with $z < 0.2$ and an [OIII] λ 5007 flux greater than 2.5×10^{-13} erg cm $^{-2}$ s $^{-1}$ (100 times lower than the limiting hard X-ray flux in SR04). All the AGN selected lie in the SR04 footprint on the sky ($|b| > 10^\circ$). This results in a sample of 55 AGN listed in Table 2 (hereafter the [OIII]-bright sample).

If the hard X-ray selected sample discussed in section 3.1 were representative of the entire AGN population, we would expect a majority of the AGN in Table 2 to be detected in hard X-rays at the flux limit of the SR04 catalog. More quantitatively, folding the [OIII]

¹We have converted all luminosities to a cosmology with $H_0 = 70$ km s $^{-1}$ Mpc $^{-1}$.

fluxes for the sample in Table 2 through the $\text{HX}/[\text{OIII}]$ flux ratio distribution for the hard X-ray selected SR04 sample in Figure 1 predicts that $\sim 70\%$ of the $[\text{OIII}]$ -bright sample (38 objects) should be detected in hard X-rays at the limit of the SR04 catalog. Instead, only 42% (23 objects) are detected. The lower-than-expected yield is entirely due to the Type 2 AGN (7 of 32, or 22%), while the Type 1 AGN are detected at the expected rate (16 of 23, or 70%). The missing Type 2 AGN are almost certainly heavily absorbed ($N_H \sim 10^{23}$ to 10^{24} cm^{-2}) or even Compton-thick ($N_H > 10^{24} \text{ cm}^{-2}$). This is consistent with the statement by SR04 that their sample contains no Compton-thick AGN, which Bassani et al. (1999) show comprise a significant fraction of Type 2 AGN.

To further investigate the hard X-ray properties of the sample, we have used literature compilations of X-ray fluxes in the 2-10 keV band (X99, Bassani et al. 1999), supplemented when necessary by our own analysis of archival data. This allows us to reach significantly lower hard X-ray fluxes than the SR04 sample, albeit in a somewhat lower energy band. These data are available for 49 of the 55 $[\text{OIII}]$ -selected AGN (6 have no published or archival hard X-ray data).

The effects of photoelectric absorption are potentially more significant in the 2-10 keV band than in the 3-20 keV RXTE band in the SR04 sample. As stated above, our goal in this paper is to compare samples of AGN selected on the basis of their observed properties (e.g. hard X-ray or $[\text{OIII}]$ flux). Thus, neither the $[\text{OIII}]$ nor the 2-10 keV fluxes we use have been corrected for absorption. For Type 2 AGN (which can often have substantial absorbing column densities) we know that we are underestimating the intrinsic hard X-ray flux. This underestimate can be as large as a factor of $\sim 10^2$ for Compton-thick AGN (e.g. Comastri 2004). We address this issue in more detail in the Appendix.

The results are shown in Figures 3 and 4. The relationship between hard X-ray and $[\text{OIII}]$ luminosities is well-behaved for the Type 1 AGN (mean ratio 1.59 dex, $\sigma = 0.48$ dex). Based on the 23 AGN in Table 2 with *both* 3-20 keV and 2-10 keV fluxes, the corresponding luminosity ratio would be 1.96 dex in the 3-20 keV band (similar to the value 2.14 dex for Type 1 AGN in the SR04/X99 sample above). A minority of the Type 2 AGN are bright in hard X-rays and overlap the range in the luminosity ratio defined by the Type 1 AGN. However, the Type 2 AGN as-a-whole are significantly weaker in hard X-rays, and the range in the $\text{HX}/[\text{OIII}]$ luminosity ratio is much larger (mean = 0.57 dex and $\sigma = 1.06$ dex) compared to the Type 1 AGN.

We therefore conclude that while the hard X-ray *vs.* $[\text{OIII}]$ properties of Type 1 AGN are relatively insensitive to the selection criteria, most optically selected Type 2 AGN are significantly weaker in hard X-rays than their counterparts in a hard X-ray selected sample. This is qualitatively consistent with earlier investigations of Type 2 AGN, which documented

the existence of a significant population of X-ray-faint AGN (e.g. Bassani et al. 1999; Risaliti, Maiolino, & Salvati 1999). We emphasize again that this does not imply that these AGN are *intrinsically* weak hard X-ray emitters. Instead, they are heavily absorbed or even Compton-thick AGN in which only a small fraction of the emitted hard X-rays are observed (Comastri 2004; Levenson et al. 2002).

4. Comparison of Hard X-ray and [OIII] Luminosity Functions

We have shown above that there is a good correlation between the [OIII] and hard X-ray luminosities for a hard X-ray selected sample of AGN. However, this is not the case for sample of AGN with bright [OIII] line emission: many of the Type 2 AGN in this sample are far weaker in hard X-rays than Type 1 AGN with the same [OIII] luminosity. To gain insight into which of the samples is more representative of the local AGN population, in the present section we compare the independently determined hard X-ray and [OIII] luminosities functions for AGN in the local universe.

SR04 have used the XSS to derive a local ($\langle z \rangle = 0.034$) hard X-ray (3-20 keV) luminosity function for Compton-thin AGN (excluding BL Lac objects). Hao et al. (2005b) used a local ($\langle z \rangle \sim 0.1$) AGN sample extracted from the SDSS to derive the [OIII] λ 5007 luminosity function. We compare these two luminosity functions in Figure 5. ²

The hard X-ray and [OIII] luminosity functions have similar slopes. To align the two functions in luminosity at fixed space density requires an offset in the luminosity scale (HX/OIII) by 1.53 to 1.68 dex (depending the assumed incompleteness correction applied to the SR04 sample - see SR04 for details). This ratio is significantly less than the mean value we have measured above for $\log(L_{HX}/L_{OIII}) = 2.15$ for individual hard X-ray selected AGN in the SR04 sample itself. Alternatively, if we fix the luminosity ratio at 2.15 dex, then at the same equivalent luminosity the space density of hard X-ray selected AGN is lower than that of [OIII]-selected AGN by a factor of ~ 0.5 dex. These results are consistent with a significant population of [OIII]-bright AGN that are relatively weak in the hard X-ray band.

²We have used the evolutionary parameters measured by B05 to slightly adjust the SR04 luminosity function to the mean redshift of the SDSS sample.

5. Luminosity Dependent Properties

Deep X-ray surveys find that objects classified optically as Type 1 AGN are a minor component of the hard X-ray selected AGN population at low luminosities (below $L_{HX} \sim 10^{43.5}$ erg/s). As noted in the introduction, there have been several different interpretations of this result, ranging from the emergence of a new type of AGN to the effects of aperture dilution in the optical spectra. Since the AGN in the SR04 sample are so much nearer and brighter, they provide an opportunity to test these interpretations.

Notably, the demographics of the SR04 sample are very different than in the B05 deep X-ray survey: for $L_{HX} < 10^{43.5}$ erg/s, the SR04 sample contains roughly equal numbers of optically-classified Type 1 and Type 2 AGN (18 *vs.* 17 objects). Could this difference be the result of cosmic evolution in the AGN population? If so, this evolution must have occurred very recently, since the apparent lack of low luminosity Type 1 AGN in the deep surveys persists even in the lowest redshift range investigated in B05 ($z = 0.1$ to 0.4).³

The difference in the Type 1 AGN fraction between SR04 and the deep X-ray surveys is consistent with the idea that many low luminosity Type 1 AGN are not recognized as such in the deep surveys because of severe dilution of the optical spectra by light from the host galaxy (Moran, Filippenko, & Chornock 2002; Severgnini et al. 2003). Moreover, Silverman et al. (2005) also show that whether or not a hard X-ray source is classified optically as a Type 1 AGN can depend sensitively on which portion of the rest-frame spectrum is observed (e.g. a Broad Line Region is much easier to recognize in the rest-frame red (with $H\alpha$) or near-UV (with $MgII\lambda 2800$) than at intermediate wavelengths where $H\beta$ is the strongest line).

B05 argue against the aperture-dilution explanation by using the high spatial resolution of HST imaging to measure a “nuclear” flux at 3000\AA (rest frame). They show that the ratio of nuclear UV to hard X-ray flux is significantly higher *in the mean* in objects classified optically as Type 1 AGNs than in the others. However, there is a very wide range in F_{UV}/F_{HX} among the objects classified optically as Type 2 AGNs (~ 3 dex), and this range overlaps that of the Type 1 AGNs. It is possible that the subset of the Type 2 AGN with high values of F_{UV}/F_{HX} are in fact misclassified Type 1 AGN.

³We emphasize that the B05 and SR04 samples do agree with one another at higher X-ray luminosities, where both are dominated by AGN classified optically as Type 1.

6. Summary

In this paper we have explored the relation between hard X-ray emission and the [OIII] λ 5007 emission line in local samples of AGN. We have used the SR04 hard X-ray (3-20 keV) selected sample of AGN, the X99 and W92 catalogs of [OIII] λ 5007 AGN luminosities, and the Hao et al. (2005b) and S04 determinations of AGN emission line and hard X-ray luminosity functions respectively to draw the following conclusions:

- For the SR04 hard X-ray selected sample of Type 1 and Type 2 AGN, the hard X-ray luminosity is well correlated with the [OIII] λ 5007 luminosity over a range of \sim four orders-of-magnitude in luminosity. The mean value for $\log(L_{HX}/L_{OIII})$ is 2.15 dex ($\sigma = 0.51$ dex). The Type 1 and Type 2 AGN have the same mean HX to [OIII] luminosity ratio (as expected in the unified model for AGN). BL Lac objects - which comprise 13% of the SR04 sample - are not included in this comparison. They would have much weaker [OIII] emission.
- For a sample of [OIII]-bright AGN derived from the X99 and W92 catalogs, the Type 1 AGN follow a hard X-ray *vs.* [OIII] luminosity relation similar to the hard X-ray selected AGN sample. However, most of the [OIII]-bright Type 2 AGN are weaker hard X-ray emitters (by an average of 1.02 dex in the 2-10 keV band) and the scatter in the HX/[OIII] luminosity ratio (1.06 dex) is much larger than for the Type 1 AGN (0.48 dex).
- The [OIII] λ 5007 luminosity function derived for optically-selected AGN from the SDSS agrees with the hard X-ray luminosity function derived for hard X-ray selected AGN for an HX/[OIII] luminosity ratio at a given space density of 1.60 dex. This is significantly smaller than the mean HX/[OIII] luminosity ratio of 2.15 dex for AGN in the SR04 sample. Alternatively - for a luminosity ratio of 2.15 dex - the space density of hard X-ray selected AGN is \sim 0.5 dex smaller than [OIII] selected AGN of the same equivalent luminosity.
- At low hard X-ray luminosities ($< 10^{43.5}$ erg/sec), the relative numbers of optically-classified Type 1 and Type 2 AGN in the SR04 hard X-ray selected sample are similar (while Type 1 AGN dominate at higher luminosities). The existence of a substantial population of Type 1 AGN with such low X-ray luminosities is not consistent with results from deep X-ray surveys. Either there has been strong cosmic evolution since $z \sim 0.1 - 0.4$, or many low luminosity Type 1 AGN are being misclassified in the deep surveys due to dilution by galaxy light in the optical spectra.

As noted in the introduction, the use of both hard X-ray and [OIII] data allows inferences to be made about the cosmic evolution of the AGN population (and its relationship to black hole growth and galaxy evolution) that in principle are more robust and physically instructive than either type of data provide in isolation.

In this context, the results above can be viewed as the classic case of a glass half full or a glass half empty. They do imply that (at least in the low-redshift universe) samples of AGN with bright [OIII] λ 5007 emission are not missing a significant fraction of the AGN selected by hard X-ray emission. Specifically, while BL Lac objects *are* weak [OIII] emitters, they comprise a distinct minority population of X-ray bright AGN (13% in SR04). The “X-ray bright, optically normal galaxies” (Levenson et al. 2001; Comastri et al. 2002; Maiolino et al. 2003; Brusa et al. 2003) are evidently not a major component of the local AGN population. This is consistent with Silverman et al. (2005) who find they comprise only 7% of the CHAMP sample (and see also Hornschemeier et al. 2005).

However (at least in the low-redshift universe), selection by hard X-rays does miss a significant fraction of the AGN population selected by the [OIII] λ 5007 optical emission-line. This population of Type 2 AGN has been long recognized (e.g. Risaliti, Maiolino, & Salvati 1999; Bassani et al. 1999), and interpreted as cases in which the hard X-ray source is heavily obscured and even Compton-thick (e.g. Levenson et al. 2002; Comastri 2004).

It is certainly possible that the class of heavily-absorbed AGN might evolve differently with cosmic time and/or trace a different population of black holes and their host galaxies and/or represent a distinct phase in the evolution of individual AGN (e.g. Wada & Norman 2002; Stevens et al. 2005). A significant population of Compton-thick AGN is required to match the overall spectrum of the cosmic X-ray background at energies above ~ 10 keV (e.g. Comastri 2004). Thus, despite the obvious advantages of hard X-ray surveys (e.g. Mushotzky 2004), it seems that multiwaveband investigations are necessary to provide a complete picture of the cosmic evolution of the AGN population and its relationship to galaxy evolution.

We thank an anonymous referee for helping us to strengthen this paper. We acknowledge the support of NASA grants NNG04GE47G and NNG04GF79G.

A. X-ray Fluxes for Absorbed AGN

Given the relatively low energy resolution of typical detectors used in X-ray astronomy, fluxes are derived in a model dependent way. A parameterized model for the X-ray spectrum

is folded through the known response of the detector and best-fit model parameters are determined through comparison to the data (e.g. Arnaud 1996). In the case of AGN, the model most commonly used is an intrinsic power law spectrum transmitted through a column density of cold gas with solar relative elemental abundances. The model fit then yields the power-law index, the absorbing column, and the flux. Fluxes are sometimes reported as-observed, and these are the fluxes listed in Table 2 and used to make Figures 3 and 4 (e.g. Bassani et al. 1999). Fluxes are also commonly reported after applying the correction for foreground absorption derived from the model fit (sometimes called “unabsorbed fluxes”).

The procedure to derive the unabsorbed fluxes are adequate for Type 1 AGN in the hard X-ray band since the absorbing columns and resulting reductions in transmitted flux are generally very small (see for example SR04). However, the methodology is often inadequate in the cases of those Type 2 AGN where absorbing columns often exceed 10^{23} cm^{-2} , and can even be Compton-thick ($> 10^{24} \text{ cm}^{-2}$). In these cases, the emerging spectrum will show the complex effects of reprocessing and radiative transfer. In well-studied cases with good X-ray spectra (e.g. Turner et al. 1997; Ogle et al. 2003), successful models require absorption by an inhomogeneous absorber (“partial covering models”), and/or reprocessing of X-rays illuminating cold or partially ionized gas, and/or electron scattering of X-rays escaping along the polar axis of the torus. When the X-ray emission from the AGN is heavily absorbed, emission from the host galaxy is often significant and adds further spectral complexity (e.g. Levenson et al. 2005). Unabsorbed fluxes derived from fitting such complex spectra with a simple absorbed power law model can significantly underestimate the true intrinsic flux - by up to a factor of $\sim 10^2$ for Compton-thick AGN (e.g. Comastri 2004).

To illustrate this, we have retrieved archival XMM-Newton X-ray spectra for 12 of the Type 2 AGN in Table 2 (NGC 526A, NGC 1068, NGC 1386, NGC 2992, NGC 4388, NGC 4507, NGC 5506, NGC 7212, NGC 7582, Mrk 1, Mrk 3, and Tol 0109-383). We have fit each spectrum with two types of models. The first is a simple absorbed power law. The second is a partial covering model in which we fit for both the absorbing column and covering fraction of the absorber. We have also added a narrow Fe $K\alpha$ line to the model, as this line can have a very large equivalent width in Compton-thick AGN (e.g. Levenson et al. 2002). This is meant to be a more physically realistic model for heavily absorbed AGN. For these AGN we find that the mean absorption correction to the hard X-ray luminosity derived from the simple power law fits is only 0.08 dex. In contrast, the mean absorption correction derived from the partial covering models is substantially larger (0.51 dex). Moreover, the intrinsic 2-10 keV luminosity as derived from the partial covering model is larger than that measured from the simple powerlaw model by 0.61 dex on-average.

The main conclusion then is that much of the large scatter seen in the ratio of the

observed hard X-ray to [OIII] fluxes in the Type 2 AGN in the [OIII]-bright sample (Figures 3 and 4) is almost certainly an artefact of absorption of the hard X-rays (see also Bassani et al. 1999). A related conclusion is that fitting simple absorbed power law models to heavily absorbed AGN significantly underestimates the intrinsic hard X-ray luminosity.

However, we emphasize that this does not affect the point we are making in this paper: we are interested in empirically assessing the effect of the bias of hard X-ray selected samples against AGN with weak *observed* hard X-ray emission. From this perspective it does not matter whether the weak X-ray emission is an intrinsic property of the AGN or just the result of severe absorption of hard X-rays. If severe enough, then it can not be properly corrected using the simple models appropriate to fitting the typical “survey-quality” X-ray spectra of AGN.

REFERENCES

- Antonucci, R. 1993, ARA&A, 31, 473
- Antonucci, R., & Miller, J. 1985, ApJ, 297, 621
- Arnaud, K., 1996, in “Astronomical Data Analysis Software and Systems V”, eds. Jacoby G. and Barnes J., ASP Conf. Series volume 101, p. 17.
- Barger, A., Cowie, L., Mushotzky, R., Yang, Y., Wang, W.-H., Steffen, A., & Capak, P. 2005 (B05), AJ, 129, 578
- Bassani, L., Dadina, M., Maiolino, R., Salvati, M., Risaliti, G., della Ceca, R., Matt, G., & Zamorani, G. 1999, ApJS, 121, 473
- Best, P., Kauffmann, G., Heckman, T., Brinchmann, J., Charlot, S., Ivezić, Z., & White, S. 2005a, MNRAS, in press (astro-ph/0506268)
- Best, P., Kauffmann, G., Heckman, T., Brinchmann, J., Charlot, S., Ivezić, Z., & White, S. 2005b, MNRAS, in press (astro-ph/0506269)
- Brinchmann, J., Charlot, S., White, S., Tremonti, C., Kauffmann, G., Heckman, T., & Brinkmann, J., 2004, MNRAS, 351, 1151
- Brusa, M., Comastri, A., Mignoli, M., Fiore, F., Ciliegi, P., Vignali, C., Severgnini, P., Cocchia, F., La Franca, F., Matt, G., Perola, G., Maiolino, R., Baldi, A., & Molendi, S. 2003, A&A, 409, 65

- Colless M. et al. , 2001, MNRAS, 328, 1039
- Comastri, A., et al. 2002, ApJ, 571, 771
- Comastri, A. 2004, in “Supermassive Black Holes in the Distant Universe”, Ed. A. Barger, Astrophysics and Space Science Library Volume 308
- Croom, A., Smith, R., Boyle, B., Shanks, T., Miller, L., Outram, P., & Loaning, N. 2004, MNRAS, 349, 1397
- Dahari, O., & De Robertis, M. 1988, ApJ, 331, 727
- Elvis, M., Wilkes, B., McDowell, J., Green, R., Bechtold, J., Willner, S., Oey, M.S., Polomski, E., & Cutri, R. 1994, ApJS, 95, 1
- Hao, L. et al. 2005a, AJ, 129, 1783
- Hao, L. et al. 2005b, AJ, 129, 1795
- Hasinger, G., Miyaji, T., & Schmidt, M. 2005, A&A, in press (astro-ph/0506118)
- Heckman, T. 1995, ApJ, 446, 101
- Heckman, T., Kauffmann, G., Brinchmann, J., Charlot, S., Tremonti, C., & White, S. 2004, ApJ, 613, 109
- Hornschemeier, A. , Heckman, T., Ptak, A., Tremonti, C., & Colbert, E. 2005, AJ, 129, 86
- Kauffmann, G. et al 2003, MNRAS, 348, 333
- Keel, W., De Grijp, M., Miley, G., & Zheng, W. 1994, A&A, 283, 791
- Kewley, L., Jansen, R., & Geller, M. 2005, PASP, 117, 227
- Krolik, J., & Begelman, M. 1988, ApJ, 329, 702
- Lawrence, A., & Elvis, M. 1982, ApJ, 256, 410
- Levenson, N., Cid Fernandes, R., Weaver, K., Heckman, T., & Storchi-Bergmann, T. 2001, ApJ, 557, 54
- Levenson, N., Krolik, J., Zycki, P., Heckman, T., Weaver, K., Awaki, H., & Terashima, Y. 2002, ApJ, 573, L81
- Levenson, N., Weaver, K., Heckman, T., Awaki, H., & Terashima, Y. 2005, ApJ, 618, 167

- Maiolino, R., Comastri, A., Gilli, R., Nagar, N. M., Bianchi, S., Bker, T., Colbert, E., Krabbe, A., Marconi, A., Matt, G., & Salvati, M. 2003, MNRAS, 344, L59
- Moran, E., Filippenko, A., & Chornock, R. 2002, ApJ, 579, L71
- Mulchaey, J.S., Koratkar, A., Ward, M.J., Wilson, A.J., Whittle, M., Antonucci, R.R.J., Kinney, A.L. & Hurt, T., 1994, ApJ, 436, 586
- Mushotzky, R. 2004, in “Supermassive Black Holes in the Distant Universe”, Ed. A. Barger, Astrophysics and Space Science Library Volume 308
- Ogle, P., Brookings, T., Canizares, C., Lee, J., & Marshall, H. 2003, A&A, 402, 849
- Revnivtsev, M., Sazonov, S., Jahoda, K., & Gilfanov, M. 2004, A&A, 418, 927
- Risaliti, G., Maiolino, R., & Salvati, M. 1999, ApJ, 522, 157
- Sazonov, S., & Revnivtsev, M. 2004 (SR04), A&A, 423, 469
- Severgnini, P. et al. 2003, A&A, 406, 483
- Steffen, A., Barger, A., Cowie, L., Mushotzky, R., & Yang, Y. 2003, ApJ, 596, L23
- Stevens, J., Page, M., Ivison, R., Carrera, F., Mittaz, J., Smail, I., & McHardy, I. 2005, MNRAS in press (astro-ph/0503618)
- Silverman, J., et al. 2005, ApJ, 624, 630
- Turner, T., George, I., Nandra, K., & Mushotzky, R. 1997, ApJS, 113, 23
- Ueda, Y., Masayuki, A., Ohta, K. & Miyaji, T. 2003, ApJ, 598, 886
- Urry, C.M., & Padovani, P. 1995, PASP, 107, 803
- Xu, C., Livio, M., & Baum, S. 1999 (X99), AJ, 118, 1169
- York D.G. et al, 2000, AJ, 120, 1579
- Wada, K., & Norman, C. 2002, ApJ, 566, L21
- Whittle, M. 1992 (W92), ApJS, 79, 49
- Wolfe, A. 1978, Ed. “Pittsburgh Conference on BL Lac Objects”, University of Pittsburgh
- Zakamska, N. et al. 2003, AJ, 126, 2125

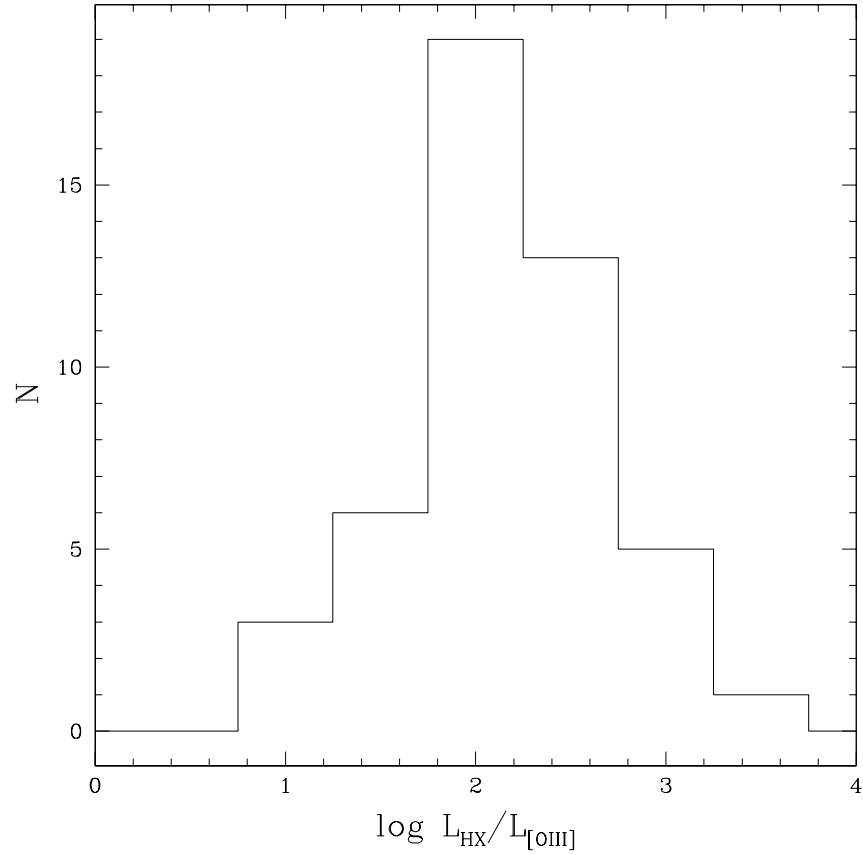


Fig. 1.— A histogram of the log of the ratio of the hard X-ray (3-20 keV) to [OIII] λ 5007 luminosities for a sample of 47 local AGN selected on the basis of their hard X-ray flux (the SR04 sample). The distribution has a mean of 2.15 dex and a standard deviation of 0.51 dex. There is no significant difference between the Type 1 and Type 2 AGN in this sample (see text for details).

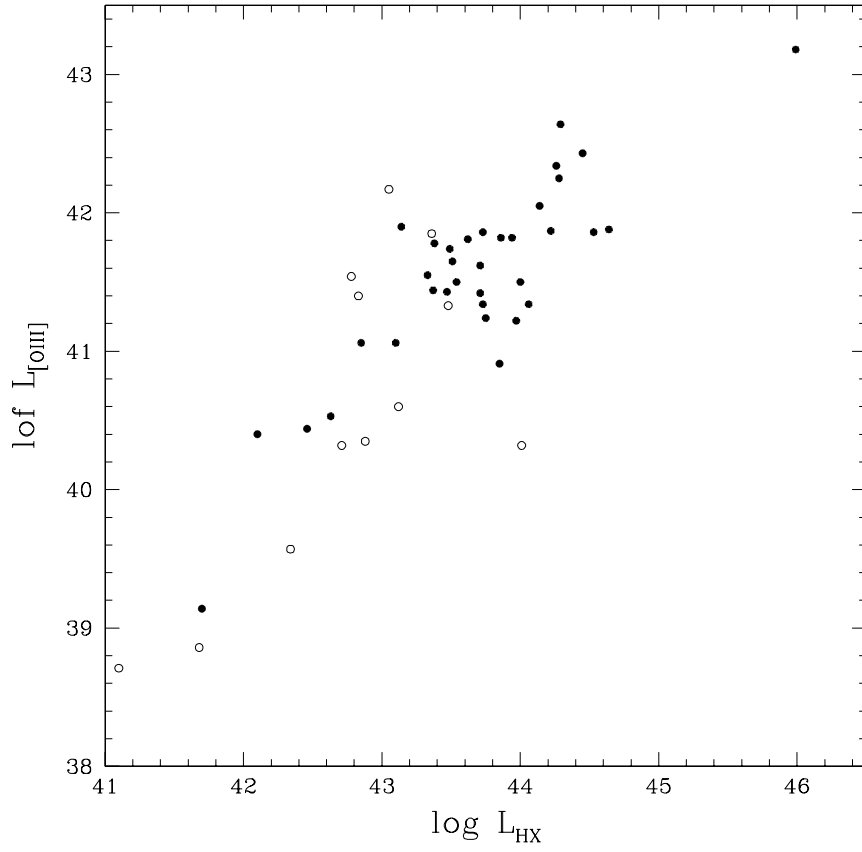


Fig. 2.— A plot of the hard X-ray (3-20 keV) *vs.* the [OIII] λ 5007 luminosities for the AGN in Figure 1. The Type 1 AGN are plotted as filled circles and the Type 2 AGN as hollow circles. Luminosities are in units of erg/sec.

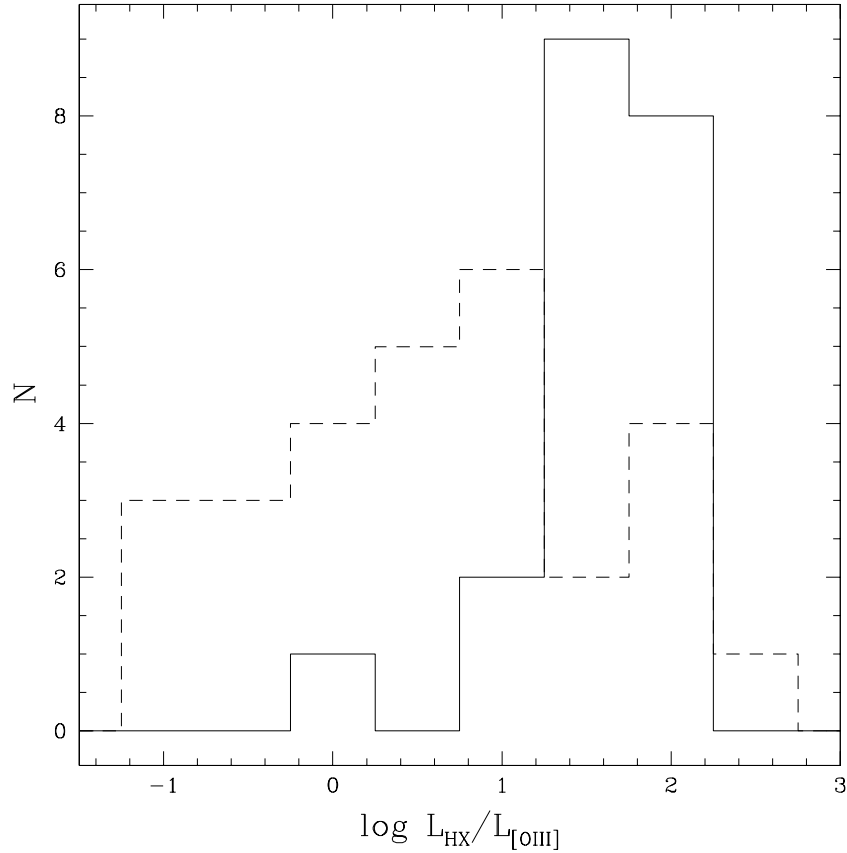


Fig. 3.— Histograms of the log of the ratio of the hard X-ray (2-10 keV) to [OIII] λ 5007 luminosities for a sample of 49 local AGN selected on the basis of their [OIII] flux (from the X99 and W92 catalogs). There is a major difference between the Type 1 AGN (solid line) and Type 2 AGN (dashed line) in this sample. For the Type 1, the mean is 1.59 dex with a standard deviation of only 0.48 dex, while for the Type 2 AGN the mean is only 0.57 dex with a standard deviation of 1.06 dex.

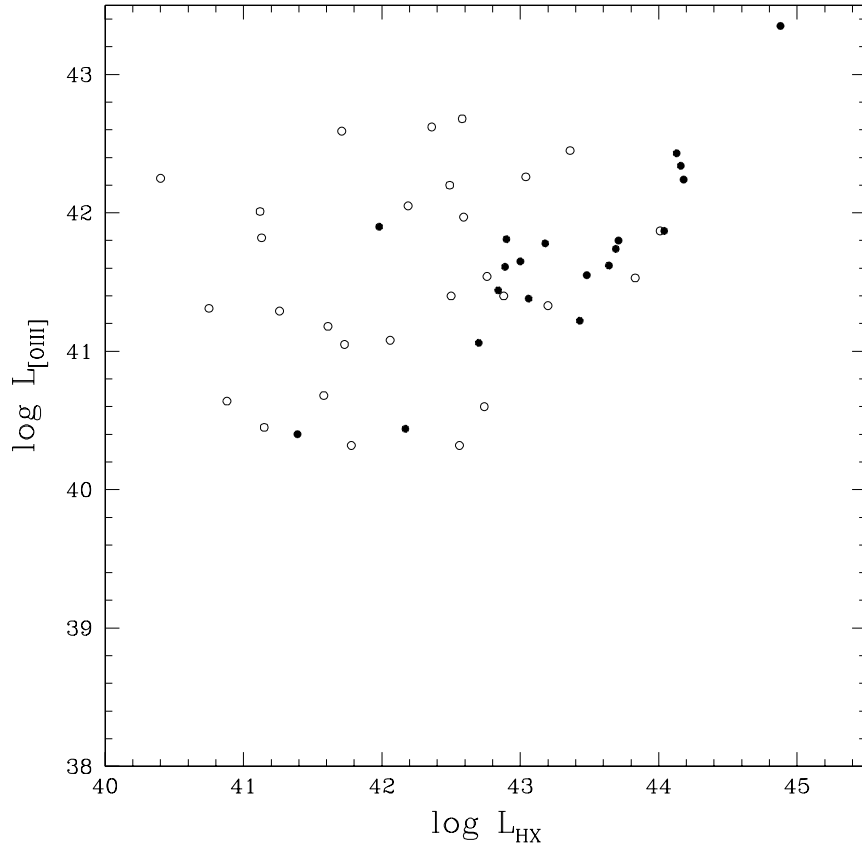


Fig. 4.— A plot of the hard X-ray (2-10 keV) *vs.* the [OIII] λ 5007 luminosities for the AGN in Figure 3. The Type 1 AGN are plotted as filled circles and the Type 2 AGN as hollow circles. Luminosities are in units of erg/sec.

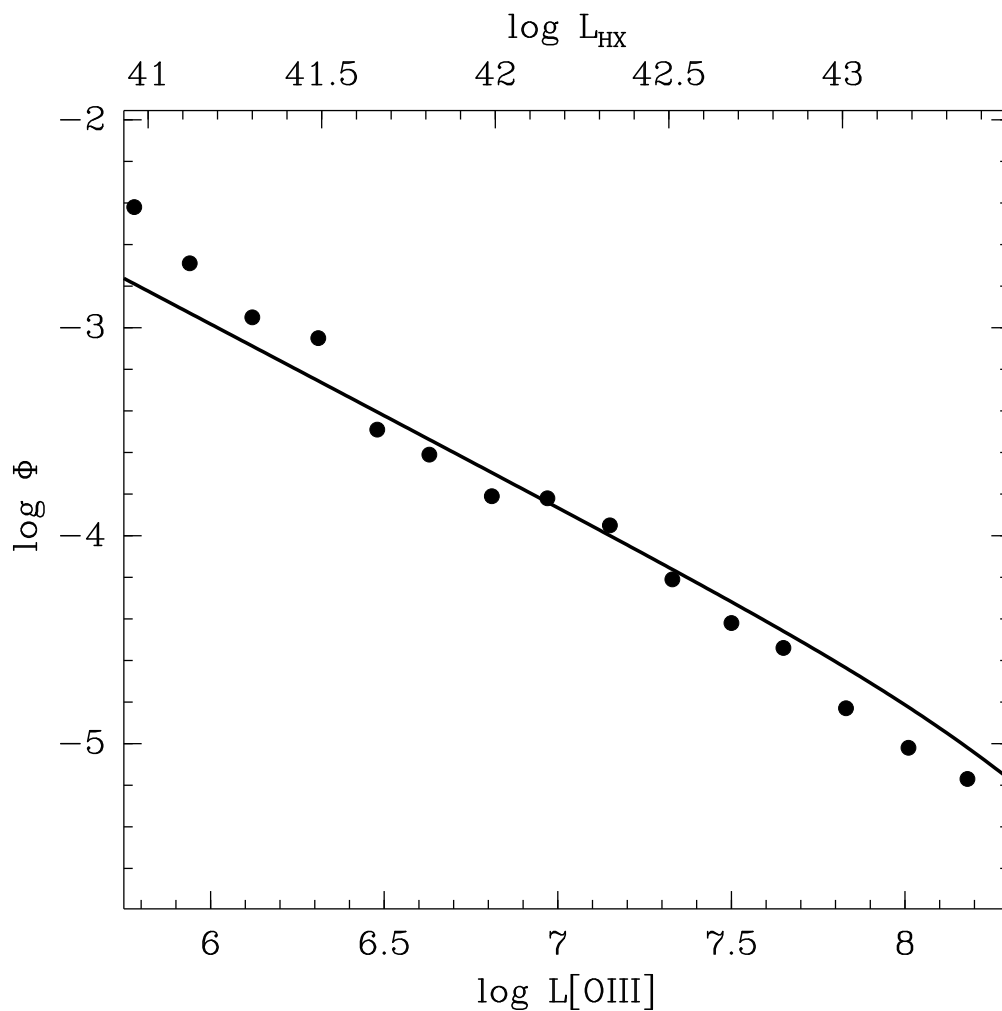


Fig. 5.— A comparison of the local AGN luminosity functions for the $[\text{OIII}]\lambda 5007$ narrow emission line (dots - from Hao et al. 2005b) and hard X-ray (3-20 keV) continuum (line - fit from SR04). Following Hao et al. (2005b) and SR04, the respective luminosities are in units of L_{\odot} for $[\text{OIII}]$ (bottom axis) and erg/sec for hard X-rays. The two luminosity functions have similar slopes, and can be aligned in space density for a luminosity ratio $\text{HX}/[\text{OIII}] = 1.60$ dex (as plotted), compared to mean ratio for hard X-ray selected AGN of 2.15 dex.

Table 1. A Hard X-ray Selected AGN Sample.

Name	Type	$\log L_{3-20}$	$\log L_{[OIII]}$
CGCG 535 – 012	1	43.54	41.50
NGC 526A	2	43.48	41.33
Fairall 9	1	44.14	42.05
Mrk 590	1	43.85	40.91
3C 120	1	44.22	41.87
Akn 120	1	44.06	41.34
Pic A	1	43.75	41.24
NGC 2110	2	42.88	40.35
MCG +8 – 11 – 11	1	43.62	41.81
Mrk 3	2	43.05	42.20
Mrk 79	1	43.51	41.65
PG 0804 + 761	1	44.53	41.86
Mrk 704	1	43.71	41.42
Mrk 110	1	43.86	41.82
MCG –5 – 23 – 16	2	43.36	41.85
NGC 3227	1	42.46	40.44
NGC 3516	1	43.10	41.06
NGC 3783	1	43.37	41.44
NGC 3998	2	41.70	39.14
NGC 4051	1	42.10	40.40
NGC 4151	1	43.14	41.90
PG 1211 + 143	1	44.28	42.25
NGC 4258	2	41.10	38.71
Mrk 205	1	43.94	41.82
NGC 4388	2	42.71	40.32
3C 273	1	46.04	43.18
NGC 4507	2	42.78	41.54
NGC 4593	1	42.63	40.53
IC 4329A	1	43.97	41.22
Mrk 279	1	44.00	41.50
NGC 5506	2	43.12	40.60

Table 1—Continued

Name	Type	$\log L_{3-20}$	$\log L_{[\text{OIII}]}$
NGC 5548	1	43.71	41.62
Mrk 841	1	43.73	41.86
Mrk 290	1	43.49	41.74
NGC 6300	2	41.68	38.86
3C 382	1	44.64	41.88
3C 390.3	1	44.45	42.43
ESO 140 – G043	1	42.85	41.06
Mrk 509	1	44.26	42.34
IC 5063	2	42.83	41.40
NGC 7314	2	42.34	39.57
Mrk 915	1	43.38	41.78
Akn 564	1	43.47	41.44
NGC 7469	1	43.33	41.55
Mrk 926	1	44.29	42.24
PG 2304 + 042	1	43.73	41.34
NGC 7582	2	44.01	40.32

Note. — Based on observed hard X-ray fluxes (3–20 keV band) from SR04 and [OIII] λ 5007 data from X99 and W92 (with no correction for intrinsic dust extinction). All luminosities are in units of erg sec^{-1} , and we take $H_0 = 70 \text{ km sec}^{-1} \text{ Mpc}^{-1}$.

Table 2. An [OIII] λ 5007 Bright AGN Sample.

Name	Type	$\log L_{3-20}$	$\log L_{2-10}$	$\log L_{[OIII]}$
NGC 526A	2	43.48	43.20	41.33
NGC 1068	2	<41.90	41.13	41.82
NGC 1275	2	<43.23	43.83	41.53
NGC 1386	2	<42.07	39.59	40.59
NGC 1566	1	<42.03	—	40.11
NGC 1685	2	<43.10	40.40	42.25
NGC 2273	2	<42.52	40.88	40.64
NGC 2992	2	<42.52	42.06	41.08
NGC 3081	2	<42.58	41.26	41.29
NGC 3227	1	42.46	42.17	40.44
NGC 3516	1	43.10	42.70	41.06
NGC 3783	1	43.37	42.84	41.44
NGC 4051	1	42.10	41.39	40.40
NGC 4151	1	43.14	41.98	41.90
NGC 4388	2	42.71	42.56	40.32
NGC 4507	2	42.78	42.76	41.54
NGC 5506	2	43.12	42.74	40.60
NGC 5548	1	43.71	43.64	41.62
NGC 5643	2	<41.95	41.15	40.45
NGC 5728	2	<42.73	41.61	41.18
NGC 7212	2	<43.59	42.19	42.05
NGC 7469	1	43.33	43.48	41.55
NGC 7582	2	44.01	41.78	40.32
Mrk 1	2	<43.19	40.75	41.31
Mrk 3	2	43.05	42.49	42.20
Mrk 6	1	<43.80	42.90	41.81
Mrk 34	2	<44.15	41.71	42.59
Mrk 78	2	<43.88	—	42.24
Mrk 79	1	43.51	43.00	41.65
Mrk 270	2	<42.64	41.58	40.68
Mrk 290	1	43.49	43.69	41.74
Mrk 348	2	<43.09	42.88	41.40
Mrk 463	2	<44.15	42.36	42.62
Mrk 477	2	<43.89	42.58	42.68
Mrk 509	1	44.26	44.16	42.34
Mrk 533	2	<43.67	42.59	41.97
Mrk 573	2	<43.21	41.12	42.01
Mrk 595	1	<43.57	42.89	41.61
Mrk 766	1	<42.95	43.06	41.38
Mrk 915	1	43.38	43.18	41.78
Mrk 926	1	44.29	44.18	42.24
Mrk 1388	2	<43.40	—	41.47
IC 4329A	1	43.97	43.43	41.22
IC 5063	2	42.83	42.50	41.40
Tol 0109 – 383	2	<42.88	41.73	41.05
Tol 1351 – 375	2	<44.18	43.36	42.45

Table 2—Continued

Name	Type	$\log L_{3-20}$	$\log L_{2-10}$	$\log L_{[OIII]}$
MCG +8 – 11 – 11	1	43.62	43.71	41.81
Fairall 51	1	<43.05	—	41.06
IRAS 0107 – 03	2	<44.22	—	42.44
IRAS 0412 – 08	1	<43.91	—	42.02
PG 0119 + 22	2	<44.19	43.04	42.26
PG 1612 + 26	1	<44.98	44.88	43.35
3C 120	1	44.22	44.04	41.87
3C 390.3	1	44.45	44.13	42.43
CGCG 498 – 038	2	<43.72	44.01	41.87

Note. — The hard X-ray data in both the 3-20 keV and 2-10 keV bands are based on the observed fluxes (see text and Appendix). Upper limits in the 3-20 keV band assume the nominal XSS limiting flux of 2.5×10^{-11} erg $\text{cm}^{-2} \text{s}^{-1}$ (SR04).. The hard X-ray data in the 2-10 keV band come from the compilations in X99 and Bassani et al. (1999) or from our analysis of archival data. The $[OIII]\lambda 5007$ data come from X99 and W92. They have not been corrected for intrinsic dust extinction. All luminosities are in units of erg sec^{-1} , and we take $H_0 = 70 \text{ km sec}^{-1} \text{ Mpc}^{-1}$.